JOURNAL OF AIRCRAFT
Vol. 32, No. 1, January–February 1995

Application of Navier-Stokes Aeroelastic Methods to Improve Fighter Wing Maneuver Performance

David M. Schuster*
Lockheed Engineering and Sciences Company, Inc., Hampton, Virginia 23666

An aeroelastic analysis method, based on three-dimensional Navier-Stokes aerodynamics, has been applied to improve the performance of fighter wings operating at sustained maneuver flight conditions. The scheme reduces the trimmed pressure drag of wings performing high-*g* maneuvers through a simultaneous application of control surface deflection and aeroelastic twist. The aerodynamic and structural interactions are decoupled by assuming an aeroelastic twist mode shape and optimizing the aerodynamic performance based on this aeroelastic mode. The wing structural stiffness properties are then determined through an inverse scheme based on the aerodynamic loads and desired twist at the maneuver flight condition. The decoupled technique is verified by performing a fully coupled aeroelastic analysis. One of the more important features of this application, over and above improved maneuver flight performance, is that the wing performance at cruise conditions is not compromised. Thus, this method represents a multiple-point wing design capability utilizing computational aerodynamics methods and aeroelastic tailoring.

Introduction

FIGHTER aircraft are required to operate at a number of flight conditions ranging from relatively low-speed flight at takeoff and landing, to high-speed cruise and maneuvering flight. An important design consideration for these aircraft is the ability to perform sustained high-*g* maneuvers, requiring trimmed flight at load factors as high as 9 *g* and Mach numbers on the order of 0.9. At these conditions, the aircraft operates in a highly transonic flowfield where strong shock waves, vortex, and separated flows exist. The performance of the vehicle is very sensitive to the presence of these phenomena, and aerodynamic and structural optimization at these conditions is important to the ability of the aircraft to meet performance goals with an efficient design.

Even though the sustained maneuver design point may be one of the main performance characteristics on which the value of the aircraft is based, it may not be the most critical design factor. Fighters typically spend the majority of time and fuel cruising to and from the mission objective. Therefore, these aircraft are usually designed for efficient cruise performance, and the maneuver design point is attained through a combination of high engine thrust, and recambering the wing by deflecting leading- and trailing-edge control surfaces. This allows the aircraft to meet performance goals, but the aerodynamic inefficiency generated by this process limits the amount of time that can be spent maneuvering, and the overall effectiveness of the aircraft is degraded.

The maturation of composite materials technology has allowed designers to adopt an improved approach to this problem. Through judicious selection of materials and orientation of the composite plies, the distribution of wing bending and torsional stiffness can be virtually specified by the structural design engineer. This capability can be used to aeroelastically tailor the wing to deform to a shape that improves aerodynamic performance at a specific flight condition.

The benefit of aeroelastic tailoring has been demonstrated in a number of studies,[1] which have been performed primarily using wind-tunnel, flight test, and linear theory analyses to obtain aerodynamic loads. The development of structurally and dynamically accurate models for these simulations is extremely expensive, and the number of designs that can be effectively evaluated is very limited. Comprehensive numerical simulations of problems involving aeroelastic tailoring are limited by the availability of accurate computational aerodynamics tools. Until recently, the state-of-the-art in computational aeroelastic methods used the transonic small disturbance (TSD) potential flow theory to supply the aerodynamic loads for coupled analyses.[2,3] However, these methods have limited application to maneuvering fighter aircraft, since the small disturbance assumptions are typically invalid for flows produced by these flight conditions. Methods using aerodynamic loads computed through the solution of the inviscid Euler equations[4,5] have also been developed, but the strong viscous interactions associated with transonic maneuvering flight also limit their utility to this problem.

There have been recent advances in the development of Navier-Stokes equation-based aeroelastic methods,[6,7] and the present study applies this type of scheme to predict the performance of aircraft operating at maneuver flight conditions. The subject aeroelastic method was originally developed for analysis of fighter aircraft, and it has been previously applied to both rigid and flexible configurations operating at conditions representative of maneuvering flight.[8,9] This effort extends these analyses to numerically define flexible configurations that exhibit improved aerodynamic performance at these extreme flight conditions.

Since the above fully coupled aeroelastic procedure can be quite computationally expensive to apply in a design environment, a rationale has been developed that decouples the aerodynamic analysis from the structural analysis. This scheme models the wing for the vehicle as a flexible surface, but the deflection of the wing is specified by the designer, rather than computed interactively with the aerodynamic load. The wing deflection is manually adjusted so as to achieve optimal aerodynamic performance at the maneuver flight condition. This deflection and the aerodynamic load associated with it are used to calculate a wing bending and torsional stiffness distribution employing an inverse procedure. These stiffness distributions can then be used to assist in the design of a detailed wing structure that will aeroelastically deform to the proper geometry under transonic maneuver loading.

Received Oct. 29, 1992; presented as Paper 93-0529 at the AIAA 31st Aerospace Sciences Meeting and Exhibit, Reno, NV, Jan. 11–14, 1993; revision received March 22, 1994; accepted for publication May 10, 1994.

*Principal Engineer. Associate Fellow AIAA.

Aerodynamic Analysis Method

The aerodynamic method chosen for this research is known as the Euler/Navier-Stokes three-dimensional aeroelastic (ENS3DAE) code.[6] It solves the full three-dimensional Reynolds-averaged Navier-Stokes equations using a central finite difference algorithm. The method accepts either single- or multiple-block grid topologies, and can be run in a steady-state or time-accurate mode. Turbulence characteristics are predicted using the Baldwin-Lomax algebraic turbulence model. For brevity, the mathematical details behind ENS3DAE are omitted, and the reader is directed to Refs. 6, 8, and 9 for further information concerning the algorithm. However, before proceeding, the issue of turbulence modeling for this problem must be further addressed.

The Baldwin-Lomax turbulence model has been shown to be ineffective for computation of highly separated flowfields, and the present study anticipates these types of flows. In an attempt to simulate streamwise turbulence history effects that are not addressed by the basic model, an eddy viscosity smoothing technique, in the spirit of that described in Ref. 10, is applied in the present analyses. This modification has been previously tested in the original ENS3D program,[11] and results have displayed improved comparison with experimental data for flows involving separation. Several higher-order turbulence models and modifications of the Baldwin-Lomax model have also been formulated by numerous researchers, each displaying varying degrees of effectiveness when applied to separated flows. The majority of these schemes work well for a relatively narrow band of problems, and one is always uncertain when applying a given method to a problem for which it was not developed. Until a model that consistently produces superior results over a broad class of problems is identified, turbulence modeling will continue to be an uncertainty that must be recognized when performing these types of applications.

Geometry Selection and Preliminary Analyses

The design scheme is based on the assumption that a wing optimized for a specific flight condition is available as an initial geometry, which can be used as a basis for the transonic maneuver wing design. The Lockheed wing B[12] was chosen as a good candidate for evaluation of this design procedure since it has a geometry representative of that used on fighter aircraft, is designed for efficient transonic cruise, and wind-tunnel data exists at cruise and off-design flight conditions. The planform for this wing is shown in Fig. 1. In addition, a set of control surfaces representative of those used on a fighter aircraft are also depicted in this figure.

The wing is modeled using a single-zone C-H grid topology with 153 points wrapped around the wing and its wake (113 points on the wing surface), 33 points from the wing root to the spanwise grid boundary (21 span stations on the wing), and 33 points from the wing surface to the outer boundary. Grid convergence studies performed during the development of ENS3D indicate that this number of grid points is sufficient to capture the salient features of the flow about isolated wings. The grid points closest to the wing are located 0.0001 local chords normal to the surface. For the Reynolds number tested, this ensures that over the majority of the wing surface, at least one point will be in the laminar sublayer of the turbulent boundary layer, which is required for accurate application of the turbulence model.

At the high angles of attack and Mach numbers dictated by this application, the Navier-Stokes aerodynamic analyses using the above grid required approximately 1200 time-steps to converge to steady lift and drag values. This equates to approximately 6 h of central processor unit (CPU) time on a Cray 2 computer. Each analysis also required approximately 7,000,000 words of central memory.

To demonstrate that the method can be effectively applied to this geometry and that the grid resolution chosen is sufficient, several computations were performed and compared with experimental data. Figures 2 and 3 compare computed and experimental pressure distributions for this wing at 22 and 80% span, respectively. In these comparisons, the experimental Mach number is 0.90 and the experimental angle of attack is 3.9 deg. The Navier-Stokes computations were run at a corrected Mach number of 0.889 and an angle of attack of 3.33 deg, as suggested by Ref. 13. The Reynolds number for this case is 1.0×10^7, based on the wing mean aerodynamic chord. The comparison between the theory and experiment is very good at these conditions, which represent an off-design case for this wing. The shock location and strength are well-predicted by the viscous computation, as are the lower surface pressures. A slight discrepancy in the upper surface leading-edge suction pressures at the inboard station and the postshock pressure distribution at the outboard station are the only significant differences between the theoretical predictions and the experimental data. Comparison of other wing stations for which experimental data are available shows similar agreement, as do comparisons at lower angles of attack, which are closer to the wing design point. The data

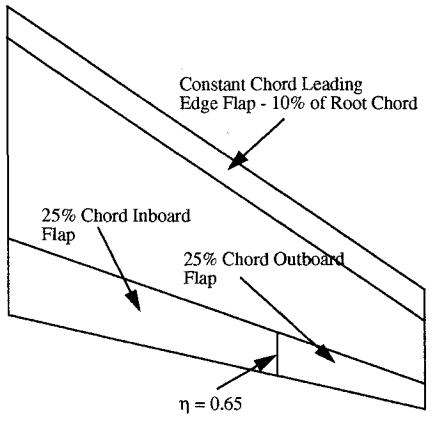

Fig. 1 Wing planform for Lockheed Wing B.

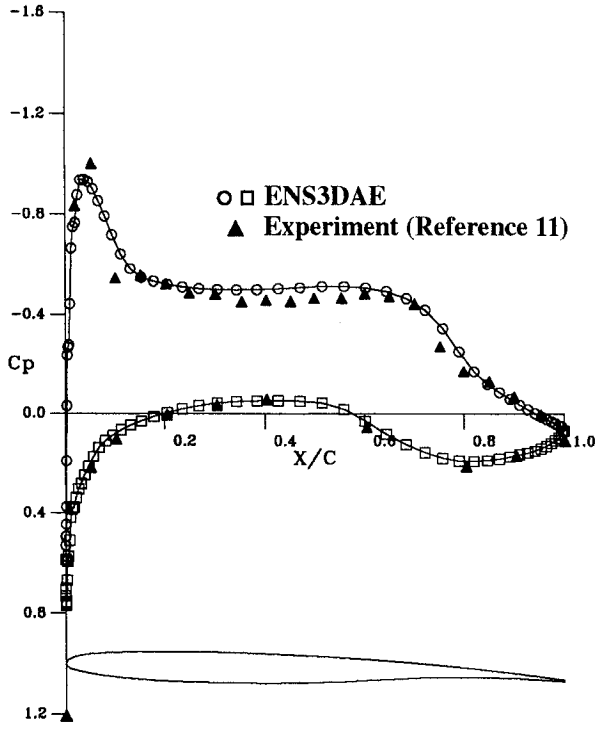

Fig. 2 Pressure distribution comparison for Lockheed Wing B, $M_\infty = 0.899$, $\alpha = 3.33$ deg, $Re = 1.0 \times 10^7$, $\eta = 0.22$.

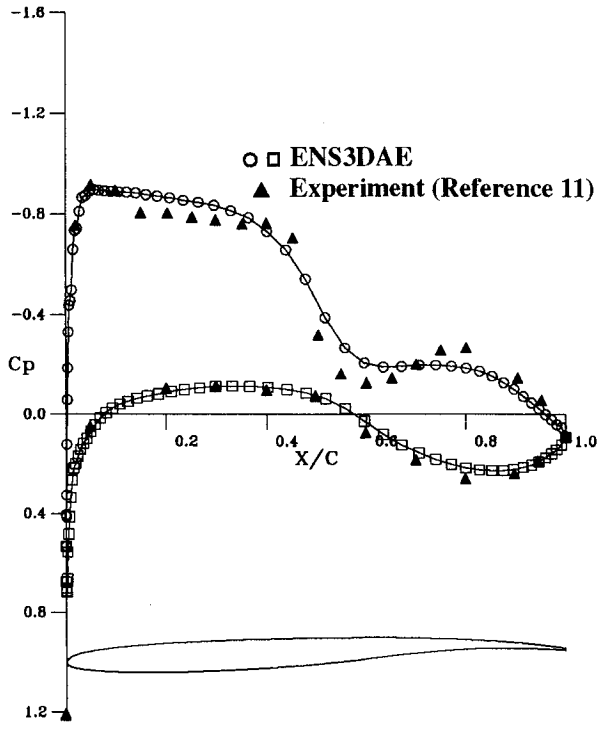

Fig. 3 Pressure distribution comparison for Lockheed Wing B, $M_\infty = 0.889$, $\alpha = 3.33$ deg, $Re = 1.0 \times 10^7$, $\eta = 0.80$.

presented here represent the highest angle of attack experimentally tested. Unfortunately, these conditions do not produce a lift coefficient that is representative of a maneuvering fighter aircraft, and the remainder of this effort is purely theoretical in nature. However, the good correlation with experiment at the wing design and off-design conditions provides incentive to apply the method at higher angles of attack.

Cruise Wing Analysis at Maneuver Flight Conditions

The basic cruise wing was next analyzed at flight conditions representative of a maneuvering fighter. A typical air superiority fighter performing a sustained 9 *g* turn at Mach 0.889- and 10,000-ft altitude requires a total lift coefficient of approximately 0.7. Therefore, these parameters were chosen as the maneuver flight conditions for this study. In addition, a transonic cruise point was also chosen to be 1 *g* flight at Mach 0.889 and 30,000-ft altitude, which requires a total lift of 0.18. The Mach number for these points was chosen so that computations at the maneuver condition would be consistent with the previous theory/experiment comparisons.

The primary figure-of-merit used to evaluate the various maneuver designs has been chosen to be the pressure drag at the maneuver lift coefficient. Typically, flight condition input to a computational aerodynamics code consists of Mach number, angle of attack, and Reynolds number. However, in this research, computations at constant lift coefficient are desired. Therefore, a simple interpolation scheme based on two computations bracketing the design lift coefficient and the assumption that the drag locally varies with the square of the lift has been developed to compute the pressure drag at the design point. Through experience, it was found that using an angle-of-attack increment of 1 deg, the design lift could be consistently bracketed in two to three aerodynamic analyses.

It is also assumed that the aircraft is operating in trimmed flight. Therefore, the pitching moment of the vehicle plays an important role in the maneuver performance. To account for this parameter, the lift and drag computed by the aerodynamic method are corrected for trim effects. This is accomplished by assuming the wing/horizontal tail combination shown in Fig. 4. From this figure, the combined wing/tail lift coefficient can be expressed through a balance of forces and moments as

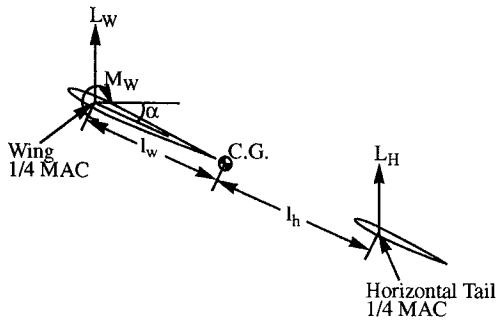

Fig. 4 Free-body diagram used to compute trim effects for a wing/horizontal tail configuration.

$$C_{L_{WH}} = C_{L_W}\left(1 + \frac{l_w}{l_h}\right) + C_{M_W}\frac{\bar{c}}{l_h \cos\alpha} \tag{1}$$

where C_{L_W} and C_{M_W} are the wing lift coefficient and pitching moment coefficient about the quarter mean aerodynamic chord, respectively, $\bar{c}$ is the wing mean aerodynamic chord, l_w and l_h are the reference lengths described in Fig. 4, and α is the angle of attack.

In addition to correcting the lift, the drag is also corrected for the presence of the horizontal tail by assuming that the drag on this surface can be approximated by

$$C_{D_H} = C_{D_{0H}} + k_H C_{L_H}^2 \tag{2}$$

where $C_{D_{0H}}$ is the zero lift drag for the horizontal tail, $K_H = (1/\pi Ae)$ for the horizontal tail, C_{L_H} is the horizontal tail lift, A is the horizontal tail aspect ratio, and e is an efficiency. Using Eqs. (1) and (2) and Fig. 4, the drag for the wing/horizontal tail combination is defined by

$$C_{D_{WH}} = C_{D_W} + K_H\left(C_{L_W}\frac{l_w}{l_h} + C_{M_W}\frac{\bar{c}}{l_h \cos\alpha}\right)^2 \frac{S_W}{S_H} \tag{3}$$

where C_{D_W} is the drag of the wing, and S_W and S_H are the planform areas of the wing and horizontal tail, respectively.

The basic cruise wing was analyzed at the maneuver flight conditions, as well as at several angles of attack between the off-design point previously presented and the maneuver flight condition. Pressure distributions from these computations indicated that the upper surface flow maintained a lambda shock pattern as for the lower lift coefficients, but at the maneuver conditions, the terminating shock separates the boundary layer on the aft portion of the wing. In an attempt to reduce the shock strength and minimize flow separation, several combinations of leading- and trailing-edge flap deflection were tested, and the results of these tests are summarized in this article.

Deflection of the leading-edge control surface only was found to be the most effective method for improving the performance of the wing at the maneuver flight condition. Figure 5 plots the drag increment between the basic cruise wing and the wing with the deflected leading-edge device as a function of the leading-edge deflection angle. Three curves are shown on this plot. The curve labeled "Untrimmed" is the drag increment obtained for the lift and drag values computed directly by the aerodynamic analysis method. The "Trimmed (Lift Only)" curve shows the drag increment when the aerodynamic loads are corrected using only Eq. (1), and the "Trimmed (Lift + Tail Drag)" curve depicts corrections applied using both Eqs. (1) and (3). In all cases, the drag increment is favorable for the 5-deg nose-down flap deflection, and unfavorable for the 10-deg deflection. A more re-

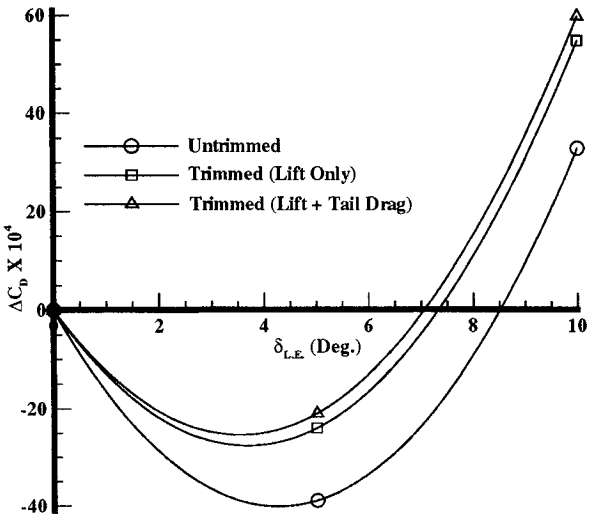

Fig. 5 Pressure drag increment due to deflection of the leading-edge control surface, $M_\infty = 0.889$, $C_{L_{WH}} = 0.7$.

fined minimum could be obtained by analyzing more flap deflections, but for this study, the 5-deg deflection exhibited the desired trend, and this deflection was chosen as the optimum for this wing. Most fighter aircraft use flap deflections to improve aerodynamic performance at maneuver flight conditions, and this demonstration represents a theoretical prediction of the performance improvements that can be expected using only this strategy. The following section describes potential improvements that can be realized by also allowing the wing to aeroelastically twist.

Wing Twist Variation to Improve Maneuver Performance

The maneuver performance improvements that can be obtained by allowing the wing to aeroelastically twist have been investigated for wing B operating at the maneuver flight condition. In the present formulation, the impact of variation of the wing twist on the aerodynamic performance is simulated, but the influence of the wing bending on the aerodynamics is neglected. The actual effects of bending are addressed in the fully coupled aeroelastic analysis presented at the end of this article.

The amount of wing twist required to obtain optimal performance is determined by systematically deforming the wing, and performing aerodynamic analyses of these twisted geometries. Since there are an infinite number of methods for twisting the wing, several assumptions were formulated regarding the form of the twist distribution, thus reducing the number of design variables to a manageable quantity.

Wing twist is usually characterized by the difference between the wingtip incidence angle and the root incidence angle, and it is safely assumed that this difference will be the dominant twist parameter impacting the aerodynamic performance of the wing. In addition, structural constraints on the wing and the nature of the aerodynamic wing loading provide a number of guidelines that aid in defining the wing twist distribution. For instance, if the wing is considered to be a cantilever beam with a fixed-end boundary condition at the wing root, then the incremental twist, as well as the slope of the spanwise twist distribution, at the root will be zero. In addition, since the aerodynamic wing loading reduces to zero at the wingtip, the curvature of the twist distribution at this point can also be assumed to be zero.

In order to ensure that these guidelines are satisfied, a scheme based on the application of normalized mode shapes to define the wing twist distribution was adopted. These mode shapes, which describe the aeroelastic twist increment between the basic wing and the flexible wing, are each defined with the above value, slope, and curvature constraints, and are normalized so that their value is either unity or zero at the wingtip. Each mode is then multiplied by a constant value that defines the increment to be added to the overall twist distribution by the given mode. Using this method, relatively complex twist distributions can be characterized by only a few design parameters.

The number of modes chosen for a given design is a tradeoff between the amount of aerodynamic improvement that can be achieved through inclusion of additional modes, and the computational resources required to perform the aerodynamic analyses associated with each mode shape. The current application uses only a single mode, and significant aerodynamic improvements are obtained utilizing this strategy. Practical issues pertaining to application of this method in a design environment will likely dictate that only a single mode be applied, even though further aerodynamic improvement may be realized by adding modes.

The mode shape chosen for this analysis is shown in Fig. 6. Rather than describe this shape using an arbitrary analytical function, such as a polynomial expression, it was extracted from historical data for an existing aeroelastically tailored geometry.[14] Thus, this mode shape has all of the basic characteristics described above, and represents a realistic aeroelastic twist distribution for an aircraft wing.

A number of computations were performed varying the amount of aeroelastic twist added to the wing at the maneuver flight condition. Figure 7 presents the drag increment between the flexible wing and the previous basic cruise wing with the 5-deg leading-edge flap deflection, as a function of the applied aeroelastic twist. Again, data are presented for both the trimmed and untrimmed load values. It is interesting to note that if the lift and drag data were not corrected for trim effects, it would appear that increasing the washout of the wing would degrade the aerodynamic performance. In reality, allowing the wing to aeroelastically twist nose down at the tip reduces the amount of load carried on the outboard section of the wing, which, for an aft-swept wing, significantly reduces the nose-down pitching moment. Thus, the horizontal tail download required to trim the aircraft is reduced and the drag penalty to trim this wing is likewise reduced.

Over 30 counts of drag improvement are realized for the fully trimmed data with approximately 4.5 deg of washout twist. Add to this the previous improvement due to the leading-edge flap deflection, and the drag increment between the flexible maneuver wing and the basic cruise wing is over 45 counts, which amounts to an overall drag reduction of approximately 5% at the maneuver flight condition. This is purely the aerodynamic benefit obtained by allowing the wing to

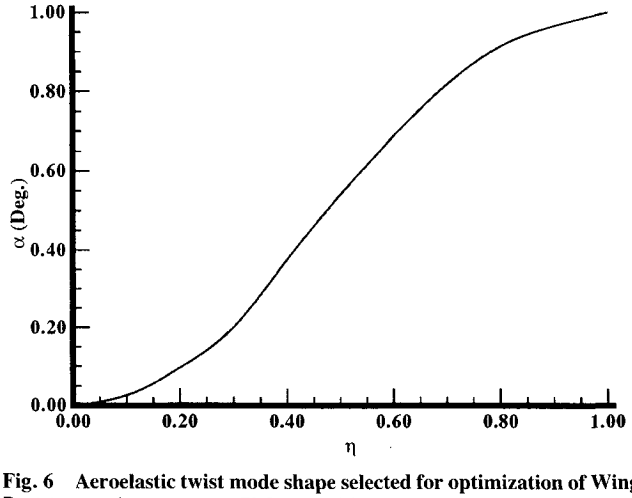

Fig. 6 Aeroelastic twist mode shape selected for optimization of Wing B at transonic maneuver flight conditions.

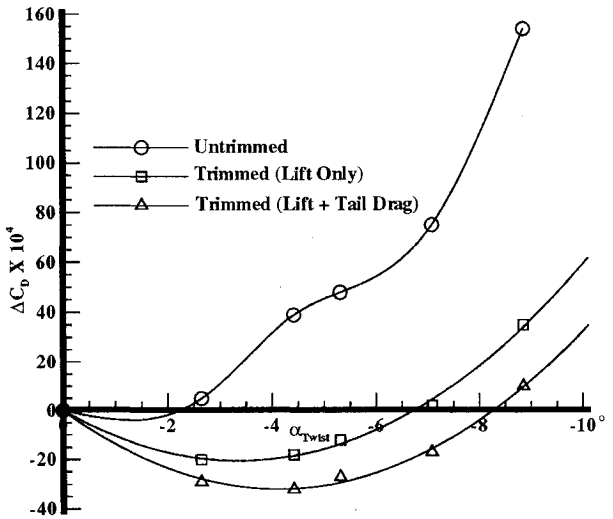

Fig. 7 Drag increment between the rigid and flexible maneuver wings operating at transonic maneuver flight conditions. $M = 0.889$, $C_L = 0.70$, $\Delta C_D = C_{D_{\text{Flex. Man.}}} - C_{D_{\text{Rigid Man.}}}$

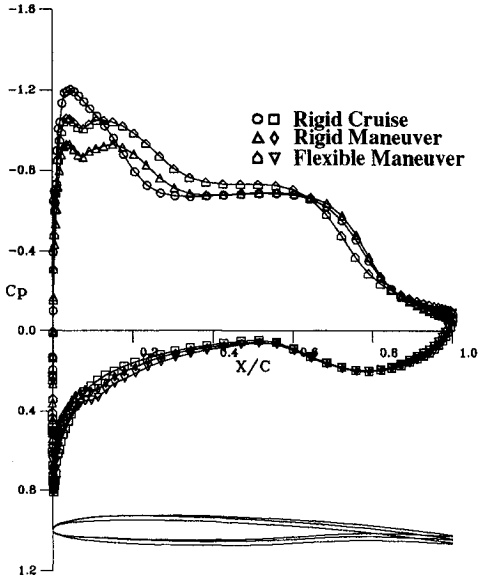

Fig. 8 Pressure distribution comparison for rigid and flexible wing designs, $M_\infty = 0.889$, $Re = 1.0 \times 10^7$, $C_{L_{WH}} = 0.70$, $\eta = 0.22$.

aeroelastically twist. In addition, there is a significant potential for savings in structural weight due to the fact that the flexible maneuver design has reduced the wing root bending moment by approximately 7.4%. The wing root torsional moment is also reduced due to the load reduction on the outer portion of the wing.

The impact of the aeroelastic twist and leading-edge flap deflection on the wing surface pressure distribution is summarized in Figs. 8 and 9. In these figures, the pressure distributions are plotted at approximately a constant trimmed lift coefficient of 0.7. The curves labeled rigid cruise denote the basic cruise wing, while those labeled rigid maneuver represent the basic wing with the 5-deg leading-edge control surface deflection, and those labeled flexible maneuver denote the rigid maneuver wing with the additional 4.5 deg of washout twist. Examining these pressure distributions, the basic effects of deflecting the leading-edge device and twisting the wing can be effectively separated and analyzed. Deflection of the leading edge control surface tends to decrease the upper surface suction on the forward portion of the airfoil, which tends to displace the terminating shock aft as compared to the rigid cruise wing. This reduces the extent of flow separation on the aft portion of the wing and adds sweep to the outboard shock. Addition of the aeroelastic twist tends to shift the aerodynamic loading to the inboard sections of the wing and reduces the shock strength on the outboard section of the wing. This inboard load shift is the primary contributor to reducing the trimmed drag increment and root bending moment for this wing.

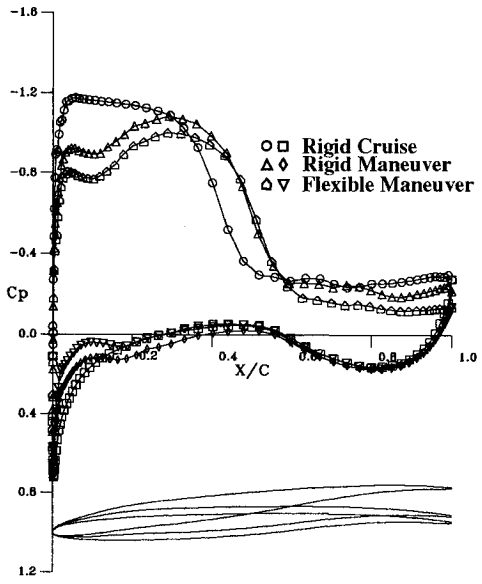

Fig. 9 Pressure distribution comparison for rigid and flexible wing designs, $M_\infty = 0.889$, $Re = 1.0 \times 10^7$, $C_{L_{WH}} = 0.70$, $\eta = 0.80$.

Calculation of the Structural Stiffness Distribution and Fully Coupled Aeroelastic Analysis

The previous computations defined a wing twist distribution and loading that result in improved aerodynamic performance at the maneuver flight condition. The final step in the design procedure is to determine the structural stiffness distribution that generates the aeroelastic twist under the computed loads. In this effort, this is done by modeling the wing as a swept beam and solving for the torsional and bending stiffness using an analytical inverse procedure. The details of this procedure are too involved to be appropriately addressed in this article, and the reader is directed to Ref. 15 for further details. Only the results of the inverse structural design will be summarized here.

The bending and torsional stiffness distributions for the wing were computed using the difference in wing loading between the basic cruise wing operating at the cruise design point and the flexible maneuver wing operating at the maneuver design point. Optimizing the stiffness using this differential loading allowed an unloaded jig shape for the wing to be computed so that at the cruise loading, the wing would aeroelastically deflect to the optimal cruise geometry, and at the maneuver loading, it would likewise deflect to the optimal maneuver geometry. Since the wing bending and torsional stiffness are dimensional quantities, the aerodynamic parameters were converted from nondimensional coefficients into dimensional loads using standard atmospheric data and geometric scalings representative of an air superiority fighter aircraft.

Figure 10 describes the bending and torsional stiffness distributions obtained using the inverse structural optimization procedure and the differential loading described above. Figure 11 compares the target twist distribution at the maneuver flight condition with the twist distribution computed using the optimized wing stiffness. The twist computed using the optimized structural stiffness distributions reproduces the target twist to within 0.05 deg over the entire wingspan.

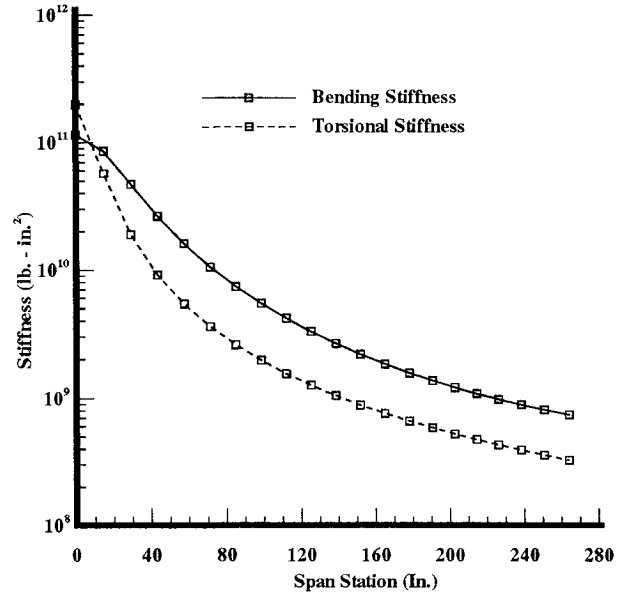

Fig. 10 Optimized bending and torsional stiffness distributions for flexible Wing B maneuver design.

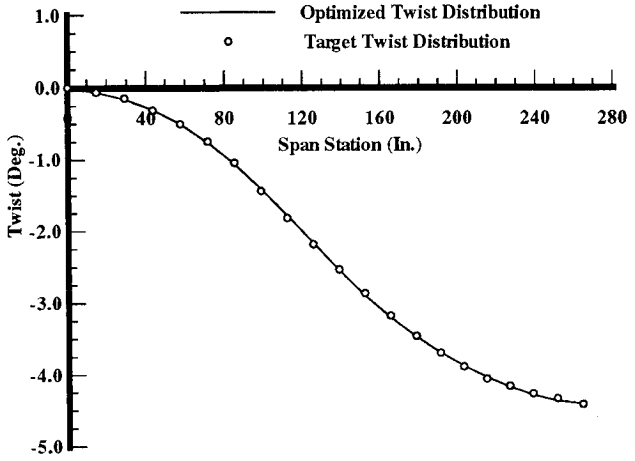

Fig. 11 Optimized and target twist distributions for flexible Wing B maneuver design.

Using the optimized wing stiffness and the cruise wing loading, the wing twist and bending for the unloaded jig shape can be accurately determined. In addition, the wing bending deflection at the maneuver design point can also be computed. Figures 12 and 13 show the twist and elastic axis bending deflection for the unloaded jig shape of the wing, the flexible cruise wing, and the flexible maneuver wing. In these figures, both the twist and deflection for the cruise wing correspond identically to the design for the basic cruise wing, whereas the twist for the maneuver wing corresponds to the optimal twist distribution defined by the aeroelastic design procedure.

To verify that the aeroelastically tailored wing will indeed deflect to the proper geometry at the transonic maneuver and cruise flight conditions, two fully coupled aeroelastic calculations were performed using the ENS3DAE aeroelastic analysis method and the optimized stiffness distributions described above. At the transonic cruise design point, the coupled aeroelastic analysis produced results that were virtually identical to the previous computations on the rigid wing. This is not surprising since the unloaded jig shape was defined so that the wing would deflect to precisely the basic cruise geometry under the cruise loading.

At the transonic maneuver design point there are slight differences in the twist distribution computed by the fully

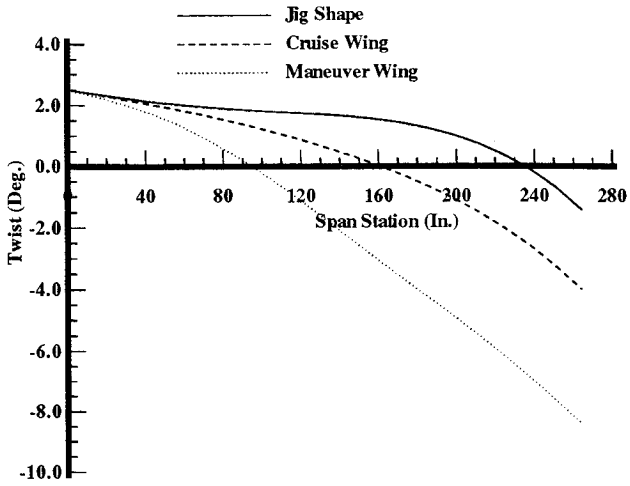

Fig. 12 Twist distributions for Wing B at unloaded, transonic cruise and transonic maneuver design points.

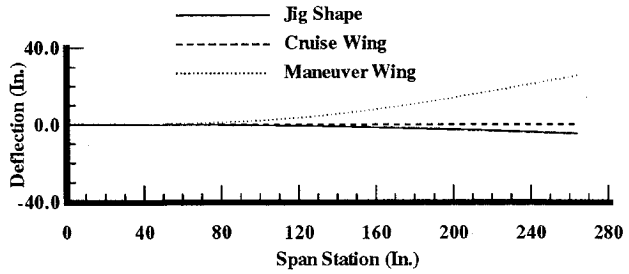

Fig. 13 Elastic axis deflection for Wing B at unloaded, transonic cruise, and transonic maneuver design points.

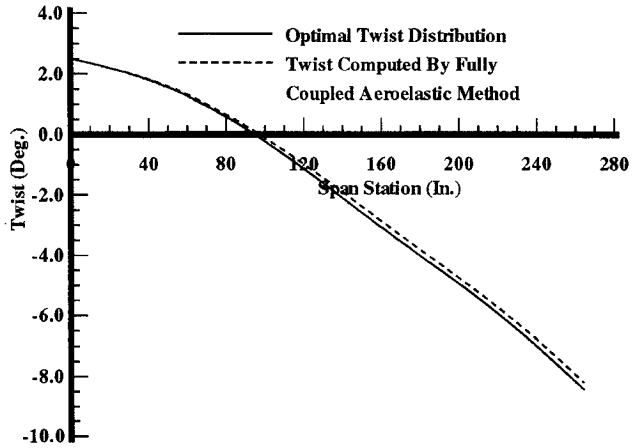

Fig. 14 Comparison of the twist distribution obtained from the coupled aeroelastic analysis and the optimal twist distribution.

coupled aeroelastic analysis and the optimal twist distribution. As shown in Fig. 14, the twist computed by the fully coupled aeroelastic analysis is slightly less than the optimal twist determined from the decoupled design. Comparison of the pressure distributions obtained from these analyses show very little difference other than that due to the small change in angle of attack at the wingtip, which indicates that the wing bending does not significantly impact the aerodynamic performance of the maneuver wing. The small differences in the twist distribution are attributed to inaccuracies in the transfer of the wing load from the aerodynamic model to the structural model in the fully coupled analysis. At present, only the vertical component of the sectional wing load is used to compute the structural deflections. However, to properly account for the wing bending, the load normal to the local wing surface should be transferred to the structural model.

Conclusions

A design rationale has been described that applies high-level computational aerodynamics methods to the aeroelastic tailoring of fighter wings operating at maneuver flight conditions. The method has been applied to a wing representative of a design that might be used on a modern fighter aircraft, and that has been previously optimized for transonic cruise flight conditions. The aerodynamic analysis method has been used to define a leading-edge control surface deflection and aeroelastic twist distribution that significantly improves the performance of the wing at transonic maneuver flight conditions. Optimal structural stiffness distributions for the wing have been defined using an inverse design method, and an unloaded jig shape for the wing has been developed so that at cruise conditions the wing will bend and deflect to the cruise design geometry, and at maneuver conditions, the wing will twist to the desired maneuver geometry. Wing bending has been neglected in the development of the maneuver twist distribution, but fully coupled aeroelastic analyses indicate that bending has effectively no impact on the aerodynamic performance of the wing. The performance of the flexible wing at the transonic cruise condition is virtually identical to that computed for the rigid transonic wing design.

There are numerous related structural and aerodynamic issues that have not been addressed in this article. Among these are the impact of reduced stiffness on structural integrity, control effectiveness, and flutter boundaries. In addition, this demonstration has been performed on a wing alone geometry using a simple swept beam structural model. In a design environment, a more appropriate structural model might be a finite element model (FEM), which would allow a tighter integration into the design process. Similar design strategies to those applied using the beam model could be incorporated in a FEM. Also, fuselage effects, especially for blended configurations, could have a significant impact on the aerodynamics of the wing and could impact the aeroelastic design. ENS3DAE is capable of analyzing these types of geometries, and with appropriate increases in computational cost, these effects could be evaluated.

Acknowledgments

The author would like to personally thank the NASA Langley Research Center, which has funded this development under NASA Contract NAS1-19000. He would also like to thank John Malone and Woodrow Whitlow of NASA Langley Research Center, and L. N. Sankar of the Georgia Institute of Technology, Atlanta, Georgia, for their support and encouragement during his pursuit of this effort.

References

[1]Shirk, M. H., Hertz, T. J., and Weisshaar, T. A., "Aeroelastic Tailoring—Theory, Practice and Promise," *Journal of Aircraft*, Vol. 23, No. 1, 1986, pp. 6–18.

[2]Borland, C. J., and Rizetta, D. P., "Transonic Unsteady Aerodynamics for Aeroelastic Applications," Air Force Wright Lab., AFWAL-TR-80-3107, June 1982.

[3]Batina, J. T., "An Efficient Algorithm for Solution of the Unsteady Transonic Small Disturbance Equations," NASA TM 89014, Dec. 1986.

[4]Guruswamy, G. P., "Unsteady Aerodynamic and Aeroelastic Calculations of Wings Using Euler Equations," *AIAA Journal*, Vol. 28, No. 3, 1990, pp. 461–469.

[5]Batina, J. T., "Unsteady Euler Algorithm with Unstructured Dynamic Mesh for Complex-Aircraft Aerodynamic Analysis," *AIAA Journal*, Vol. 29, No. 3, 1991, pp. 327–333.

[6]Schuster, D. M., Vadyak, J., and Atta, E., "Flight Loads Prediction Methods for Fighter Aircraft," Air Force Wright Lab., WRDC-TR-89-3104, Nov. 1989.

[7]Guruswamy, G. P., "Vortical Flow Computations on Swept, Flexible Wings Using Navier-Stokes Equations," *AIAA Journal*, Vol. 28, No. 12, 1990, pp. 2077–2084.

[8]Vadyak, J., and Schuster, D. M., "Navier-Stokes Simulation of Burst Vortex Flowfields for Fighter Aircraft at High Incidence," *Journal of Aircraft*, Vol. 28, No. 10, 1991, pp. 638–645.

[9]Schuster, D. M., Vadyak, J., and Atta, E., "Static Aeroelastic Analysis of Fighter Aircraft Using a Three-Dimensional Navier-Stokes Algorithm," *Journal of Aircraft*, Vol. 27, No. 9, 1990, pp. 820–825.

[10]Shang, J., and Hankey, W. L., Jr., "Numerical Solution for Supersonic Turbulent Flow over a Compression Ramp," *AIAA Journal*, Vol. 13, No. 10, 1975, pp. 1368–1374.

[11]Vadyak, J., and Smith, M. J., "Simulation of Engine Installation Flowfields Using a Three-Dimensional Euler/Navier-Stokes Algorithm," AIAA Paper 86-1537, June 1986.

[12]Hinson, B. L., and Burdges, K. P., "Acquisition and Application of Transonic Wing and Far-Field Data for Three-Dimensional Computational Method Evaluation," Air Force Office of Scientific Research, AFOSR-TR-80-0421, March 1980.

[13]Green, L., Zhang, Q., Garriz, J., Wang, S., Vatsa, V., Haigler, K., and Newman, P., "NASA/CAE Wind Tunnel Interference Cooperative Program—Status and Sample Results, January, 1991," International Conference on Adaptive Wall Wind Tunnel Research and Wall Interference Correction, ICAW 1991 Paper W-1, Xian, Shaanxi, People's Republic of China, June 1991.

[14]Miller, G. D., "Active Flexible Wing (AFW) Technology," Air Force Wright Lab., AFWAL-TR-87-3096, Feb. 1988.

[15]Schuster, D. M., "An Inverse Method for Computation of Structural Stiffness Distributions of Aeroelastically Optimized Wings," AIAA Paper 93-1540, April 1993.